Seismic response trends evaluation and finite element model calibration of an instrumented RC building considering soil-structure interaction and non-structural components

Faheem Butt

Department of Civil and Environmental Engineering, The University of Auckland, Auckland, New Zealand

Piotr Omenzetter (corresponding author)

The LRF Centre for Safety and Reliability Engineering, School of Engineering, University of Aberdeen, Aberdeen, UK

piotr.omenzetter@abdn.ac.uk

University of Aberdeen
School of Engineering
The LRF Centre for Safety and Reliability Engineering
King's College
Aberdeen, AB24 3UE
Scotland, UK
Tel. 44-1224-272529

Abstract

This paper presents experimental system identification and numerical modelling of a three story RC building monitored for a period of more than two years. System identification was conducted for 50 earthquake response records to obtain the frequencies and damping ratios considering the flexible base model that take into account soil-structure interaction (SSI). Trends of variation of modal parameters were investigated by correlating the peak response acceleration at the roof level with identified frequencies and damping ratios. A general trend of decreasing frequencies with increasing level of response was observed and quantified, whereas for damping ratios no clear trends were discernible. In the second part of the study, a series of three dimensional finite element models (FEMs) of the building were developed to investigate the influence of various structural and non-structural components (NSCs), such as cladding and partitions, as well as soil underneath the foundation and around the building, on the building dynamics. The aforementioned components were added to the FEM one by one and corresponding natural frequencies computed. The final, all-inclusive FEM was then calibrated using a sensitivity based model updating technique and experimental modal parameters by tuning the stiffness of structural concrete, soil and cladding. The updated FEM was further validated by comparing the recorded acceleration time histories to those simulated using the FEM. Finally, the updated FEM was used in time history analyses to assess the building serviceability limit state seismic performance. It was concluded from the investigations that natural frequencies depend quite strongly on the response magnitude even for low to moderate level of shaking. NSCs and SSI have been demonstrated, through both numerical models and FEM updating, to have a significant influence on the seismic response of the building. A calibrated FEM proved to be less conservative for

2

simulating seismic responses compared to the initial FEM but the building still performed satisfactorily.

Introduction

The full scale, in-situ investigations of instrumented buildings present an excellent opportunity to observe their dynamic response in as-built environment, which includes all the real physical properties of a structure under study and its surroundings. The recorded responses can be used for better understanding of behaviour of structures by extracting their dynamic characteristics (Hart and Yao 1976; Saito and Yokota 1996). Previous studies have shown that the dynamic characteristics often vary with vibration amplitude (Satake and Yokota 1996; Trifunac et al. 2001; Celebi 2006). It is, therefore, important to examine the behaviour of buildings under different excitation scenarios. The trends in dynamic characteristics, such as modal frequencies and damping ratios, thus developed can provide quantitative data for the variations in the behaviour of buildings. Moreover, such studies can provide useful information for the development and calibration of realistic models for prediction of seismic response of structures in limit state, model updating and structural health monitoring studies (Brownjohn and Xia 2000; Sohn et al. 2003).

An important factor in the analysis of civil engineering structures is the effect of soil-structure interaction (SSI) which involves the transfer of energy from the ground to the structure and back to the ground. Mathematically, SSI affects the eigensolutions of the governing equations of motion (Trifunac and Todorovska 1999). SSI effects during strong motion events were extensively studied in Celebi and Safak (1991; 1992), Safak (1993) and Celebi (2006). These studies used data from instrumented buildings and analysed them via Fourier amplitude spectra, a frequency domain technique. It was concluded that SSI, manifested in foundation rocking and beating phenomena, may have a strong influence on the response of structures subjected to strong shaking. Stewart and Fenves (1998) used a parametric system

4

identification technique to identify fixed, pseudo flexible and flexible base modal parameters for which recordings of base rocking, lateral roof motion, lateral foundation motion and free-field motion were required. They developed procedures for estimating fixed or flexible base modal parameters for the sites where limited instrumentation is available and found their method giving comparable results when using complete instrumentation. Lin et al. (2008) studied SSI with torsional coupling in building response by employing a system identification technique using information matrix. In their investigation, foundation rocking as well as translational and torsional motions of the foundation floor were used as inputs for system identification. It was concluded that all of the foundation motions should be included in the system input to avoid overestimation of actual periods.

For structural analysis of constructed systems, the finite element method is extensively used, with some important recent applications in the areas of structural health assessment and model updating (Weng et al. 2009; Wang et al. 2010; Foti et al. 2012). In each of these applications, it is necessary to understand the dynamic behaviour of a structure which depends on its modal properties. Usually, finite element models (FEMs) are constructed to estimate these properties using structural drawings, design assumptions, engineering judgment and mathematical approximations that may not represent all the physical aspects of the actual structure. Some of the important factors, for example contributions of SSI and non-structural components (NSCs) such as cladding and partition walls etc., are often ignored in FEMs. These factors, if modelled adequately in FEMs, can affect the dynamic simulations significantly, as was found, e.g., in Bhattacharya and Dutta (2004), Shakib and Fuladgar (2004), Su et al. (2005) and Pan et al. (2006). In these studies, the numerical models were either compared with each other or with the dynamic

5

characteristics extracted through ambient or forced vibrations. Usually, the plasterboard-clad walls are considered to provide no significant contribution to lateral stiffness. However, Lee et al. (2007) observed through quasi static cyclic and dynamic physical tests, that these types of walls do provide lateral stiffness and strength. Therefore, to reduce the dependence on the approximations and better replicate the true behaviour of structures, all influential structural and non-structural components should be modelled in FEMs. This study uses the responses of a full scale instrumented building recorded during actual earthquakes and finite element simulations to investigate the contributions of SSI and NSCs (cladding and partition walls) to the building seismic dynamics.

Although finite element modelling is an efficient tool, reproducing very accurately the measured dynamic characteristics is a considerable challenge (Brownjohn et al. 2001a). To improve the response prediction of an FEM, it is important to update or calibrate it with respect to the measured actual response. Iterative model updating methods are particularly advantageous because they apply corrections to local physical parameters of the FEM and their updated results are physically interpretable. Further general details on model updating techniques can be found in Friswell and Mottershead (1996). Representative approaches include the optimal matrix updating, sensitivity based parameter estimation, eigenstructure assignment algorithms and neural-networks updating methods (Zhang et al. 2000). A brief introduction to the sensitivity based parameter estimation method will be presented later in this paper as this method is used in the study.

This study comprises two parts. In the first part, a review of the seismic response trends of an instrumented RC building evaluated using 50 recorded earthquake time histories collected over a period of more than two years is presented.

Natural frequencies and damping ratios were identified taking into account SSI. Relationships and trends between the identified natural frequencies and damping ratios and peak response acceleration (PRA) at the roof level were studied via rigorous statistical analysis using a relatively large number of seismic events. The purpose of this part of the paper is to highlight the variability of, and trends in, modal properties and provide a context for subsequent numerical analyses of the building.

The second part of this investigation includes the development of a series of FEMs to which structural and non-structural components and soil flexibility were added one by one to study their contributions to the modal characteristics of the building. The frequencies and mode shapes produced by the final, all-inclusive FEM were compared to those experimentally identified from the measured responses to the strongest recorded earthquake. The differences observed were then minimized by model updating using a sensitivity based technique. The updated model was used for serviceability limit state assessment of the building under a selection of 10 ground motion records obtained at the site and appropriately scaled. This part contributes to better understanding of the importance of modelling the soil and NSCs to simulate the real dynamic behaviour of building structures. Another contribution is the calibration of the FEM including SSI and NSCs and the use of an experimentally benchmarked model for assessment of structural performance which is rare in the existing literature.

Overall, the paper furthers the understanding of dynamic behaviour of buildings during earthquakes and provides new methods and quantitative data for studying seismic responses of as-built structures, structural health monitoring and model updating. The limitation is, however, that only low to medium intensity seismic records were available. Consequently, only linear structural models were adopted. To extend the present study, possibly into non-linear range, more data, including those

from high intensity earthquakes, are required but are currently not available for the building. The analysed excitation level is, nevertheless, of interest and importance for serviceability limit state studies where structures remain in their elastic, linear or only mildly non-linear, range. For example Uma et al. (2010) studied the effect of seismic actions on acceleration-sensitive NSCs and concluded that the acceleration demands for NSCs can increase even in the lesser intensity shaking, which can damage them and consequently disrupt operational continuity of buildings. Therefore, a wide range of ground shaking intensities, from low to high, and the corresponding dynamic behaviour of structures should be considered in design to avoid such damage and operational disruption. Also, to account for the time dependent variation of structural response due to aging, environmental agents and consequently degradation of RC structures, the responses to both ultimate and serviceability limit state shaking should be evaluated (Berto et al. 2009). Furthermore, low to medium shaking levels are important as the baseline data to judge the condition of the structure in structural health monitoring applications (Sohn et al. 2003).

Description of the building and instrumentation

The structure under study is the GNS Avalon building situated in Lower Hutt, approximately 20km North-East of Wellington, New Zealand. The layout of the building and instrumentation is shown in Figure 1a and b. It is a three story RC structure with a basement, 44.70m long, 12.19m wide and 13.40m high (measured from the base level). The structural system consists of seven two-bay moment resisting frames of spans 5.33m and 6.86m, respectively, and a 2.54m×1.95m RC shear core with the wall thickness of 229mm, which houses an elevator. The plan of the building is rectangular but the presence of the shear core, irregularity of frame spacing near the shear core, unequal frame bay spans and, to a much lesser degree, the

8

staircase and the beams along the longitudinal direction inside the perimeter beams, makes it unsymmetrical in terms of structural stiffness distribution (Figure 1a). All the beams and columns are of rectangular cross-section. The exterior beams are 762×356mm except at the roof level where these are 1067×356mm. All the interior beams and all the columns are 610×610mm. Floors are 127mm thick RC slabs except for a small portion of the ground floor near the stairs where it is 203mm thick. The roof comprises corrugated steel sheets over timber planks supported by steel trusses. The columns are supported on pad type footings of base dimensions 2.29×2.29m on the perimeter and 2.74×2.74m inside the perimeter, and 610×356mm tie beams are provided to join all the footings together.

The building is instrumented as part of the New Zealand's GeoNet Structural Array (GeoNet 2013). The instrumentation comprises five tri-axial accelerometers. Two accelerometers are fixed at the base level, one underneath the first floor slab, and two at the roof level as shown in Figure 1b. There is also a free-field tri-axial accelerometer mounted at the ground surface on a concrete pad and located 39.40m from the building. Figures 1a and b also show the common global axes X and Y used for identifying directions in the subsequent discussions.

System identification for evaluating SSI effects

For incorporation and evaluation of SSI effects using system identification procedures, Stewart and Fenves (1998) proposed the following approach. Consider the structure shown in Figure 2. The height h is the vertical distance from the base to the roof (or another measurement point located on the building). The symbols denoting translational displacements are as follows: u_g for the free-field translational displacement, u_f for the foundation translational displacement with respect to the free field, and u for the roof translational displacement with respect to the foundation

resulting from inter-story drift. Foundation rocking angle is denoted by θ, and its contribution to the roof translational displacement is $h\theta$. The Laplace domain counterparts of these quantities are denoted as $\hat{u}_g$, $\hat{u}_f$, $\hat{u}$ and $\hat{\theta}$, respectively.

Stewart and Fenves (1998) consider the following flexible base transfer function:

$$ H = \frac{\hat{u}_g + \hat{u}_f + \hat{u} + h\hat{\theta}}{\hat{u}_g} \tag{1} $$

where input is the free-field displacement u_g and output is the total roof displacement $u_g+u_f+u+h\theta$. They demonstrated that the poles of the flexible base transfer function H give natural frequencies and damping ratios of the entire dynamical system comprising the structure, foundation and soil. In other words, the identified modal parameters are influenced by the stiffness and damping of soil. To provide a simple quantification of the effects of SSI on the response of the building, modal vibration parameters were sought using the N4SID technique (Van Overschee and De Moor 1994) for the flexible base case with input-output pairs consisting of a combination of free-field, foundation and superstructure level recordings as explained in Equation (1). In this study, accelerations measured by sensor 10 (the free-field sensor) in all three directions was considered as the input and accelerations measured by sensors 3, 4, 5, 6 and 7 as the outputs for the flexible base case. Stability diagrams (Bodeux and Golinval 2001) were used for the N4SID to eliminate spurious results due to measurement errors.

Evaluation of seismic response trends including SSI effects

The objective of this part of paper is to present the seismic response of the building under a large number of earthquakes of different strength. Of particular interest are the trends between PRA and the identified first three natural frequencies and

10

corresponding damping ratios of the building observed in 50 different earthquakes. The presentation of this part of the study comprises the selection of earthquakes, modal system identification and correlating the PRAs with the identified frequencies and damping ratios for flexible base models. It is noted that the results reported in this part are a selection from a more extensive study conducted recently (Butt and Omenzetter 2012) that included also another building and attempted to separate SSI effects on the building dynamics. Their inclusion in this paper serves the purpose of completeness and highlighting the variability of the identified modal parameters as well as setting the context for the subsequently reported finite element modelling and model updating that only consider a single ground motion.

For this study, 50 earthquakes recorded on the building between November 2007 and February 2010 which had epicentres within 200km from the building were selected. The reason for this was to select earthquakes of such an intensity that could excite the modes of interest with acceptable signal-to-noise ratios providing quality system identification results. The area surrounding the building had not been hit by any strong earthquake since its instrumentation. The recorded earthquakes had a moment magnitude ranging between $M_W = 3.0$ and 5.0, with most of them clustered at the lower end of this interval. This means that nearly all of the earthquakes fell into the category of low intensity except for a very few that can be treated as moderate events.

Table 1 summarizes maximum accelerations recorded at the free field, base and roof sensors for the 50 earthquakes. The maximum peak ground acceleration (PGA) at the free-field sensor 10 was recorded along Y-direction (0.0138g) and was almost double the maximum along X-direction (0.0074g). The maximum PGA at the base of the building was 0.0092g and was captured by sensor 6 along Y-direction, and

11

was a little higher than the maximum PGA recorded by sensor 7 along Y-direction (0.0090g). Along the X-direction, sensor 7 recorded a slightly higher maximum PGA (0.0061g) than sensor 6 (0.0059g). The maximum PRA of the building in the Y-direction was 0.0412g captured by sensor 4, which was double the maximum recorded acceleration in the X-direction of 0.0206g. For sensor 3, the maximum PRA was a little lower (0.0390g) as that of sensor 4 along the Y-direction and almost double its own maximum PRA in the X-direction (0.0185g). It should be noted, however, that the majority (94%) of analysed earthquakes resulted in PRAs below 0.015g (this will also be seen clearly later in Figure 4).

The following paragraphs report on the results of modal identification of the building using the selected 50 earthquake records. The typical first three mode shapes of the building are shown in Figure 3 in planar view. (Note that because of a limited number of measurement points those graphs assume the floors and all foundation pads connected by tie beams move as rigid diaphragms.) The shape of the first mode shows it to be a translational mode along X-direction with some torsion. The second mode is translationally dominant along Y-direction coupled with torsion, and the third one is torsionally dominant with some Y-direction translation present. Structural irregularities, such as those due to the shear core present near the North end of the building, irregular frame pattern near the shear core, unequal frame bay spans and, to a lesser degree, staircase and internal longitudinal beams being not in the middle, create unsymmetrical distribution of structural stiffness which causes the modes to be coupled translational-torsional. Another plausible source of mode shape coupling may be varying soil stiffness under different foundations and around different parts of the building. (Note, however, that in all the numerical simulations presented later such spatial soil variability is ignored.)

12

Table 2 shows the minimum, maximum, average and relative spread (= (maximum-minimum)/average×100%) values of the identified modal frequencies for the analysed 50 earthquakes for the flexible base model. The average first three modal frequencies for the building are 3.33Hz, 3.61Hz and 3.79Hz and the relative spreads are 14%, 19% and 11%, respectively. Figures 4a and b show the results of modal frequency identification for the analysed 50 earthquakes. The frequencies are plotted against PRAs in X- and Y-direction of a representative roof sensor (sensor 3). It can clearly be seen that modal frequencies decrease as the PRAs increase and this is observed for all three modes, and along both X- and Y-directions. In order to quantify relationships between PRAs and modal frequencies linear regression was applied (Montgomery et al. 2001). In Figures 4a and b the formulas relating the identified modal frequencies and PRA in both X- and Y-direction are listed (y stands for a frequency in Hz and x for PRA in g). The negative values of the linear terms confirm again the decreasing trend of modal frequencies with increasing PRA. The strength of correlations of the variables is illustrated by R^2 or coefficient of determination (Steel and Torrie 1960). The coefficients of determination vary from 0.33 to 0.65 indicating that a linear relationship fits the data to a reasonable degree. Had more data with PRAs in the range beyond 0.01g been available it would have helped to develop more refined relationship than the linear one.

Table 2 also shows the minimum, maximum, average and relative spread values of the identified modal damping ratios for the analysed 50 earthquakes for the flexible base model. The average values of damping ratios for the first, second and third mode are 3.4%, 5.6% and 3.1%. It can be noticed that the identified damping ratios show considerable scatter – the relative spreads are between 176% and 240%. Such large spreads may be the result of both actual variability of damping as well as

errors introduced by the identification method, and generally confirm observations from past full scale identification exercises where the uncertainties in damping identification were considerably higher than those of frequencies (see, e.g., Brownjohn et al. 2003). No clear trends in dependence of the damping ratios on PRA could be discerned.

Study on the influence of structural and non-structural components and soil stiffness on the building dynamics using FEM

Development of the FEM in stages and modelling of structural components

To evaluate the effect and contribution of structural and non-structural components and SSI, a series of three dimensional FEMs was developed using available structural drawings and additional at-site measurements and inspections. The following series of FEMs were considered in the study:

- Stage I: Bare, fixed base, three-dimensional frame with masses of slabs, dead and live loads lumped at the nodes;

- Stage II: Fixed base frame with slabs and stairs modelled and dead and live loads applied to them;

- Stage III: As in Stage II with shear core (lift shaft) added;

- Stage IV: As in Stage III with NSCs (partition walls and cladding) modelled;

- Stage V: As in Stage IV with soil underneath foundation modelled; and

- Stage VI: As in Stage V with soil around the building modelled.

ABAQUS (2011) software was used for modelling. The beams and columns were modelled using Timoshenko beam elements (designated as B31), and slabs, stairs and shear core using four-node, first-order shell elements (designated as S4). Linear elastic material properties were considered for the analysis. Initially the

columns were assumed to be fixed to the ground and beam to column connections were also assumed as fixed (moment resisting frame assumption). The density and modulus of elasticity of RC for all the elements was taken as 2400kg/m^3 and 30GPa respectively. The steel density and modulus of elasticity for roof elements were taken as 7800kg/m^3 and 200GPa, respectively. The steel trusses present at the roof level were modelled as equivalent steel beams, having the same mass and longitudinal stiffness, using beam B31 elements. The masses of the timber purlins, planks and corrugated steel roofing were calculated and lumped at the equivalent steel beams. The mass due to partition walls, false ceilings, attachments, furniture and live loads was collectively applied at the floor slabs as area-distributed mass of 450kg/m^2 according to design recommendations (ASCE/SEI 7-05 2005).

Modelling of NSCs

Since the structure under study is an office building, there are a large number of partition walls present. The partitions were modelled as two node SPRING2 diagonal elements. The stiffness value of those springs was taken from Kanvinde and Deierlein (2006) as 2800kN/m. External cladding in the building is made up of fiberglass panels with insulating material on the inner side. The density and modulus of elasticity values of fiberglass were taken as 1750kg/m^3 and 10GPa, respectively, from Gaylord (1974) and their mass was calculated manually (100kg/m) and applied at the perimeter beams.

Modelling of SSI

The soil present at the building site is classified according to the New Zealand Standard 1170.5 (Standards New Zealand 2004) as class D (deep or soft soil). The

shear wave velocity, V_s, was taken as 160m/s based on the investigation for the site subsoil classification (Boon et al. 2011), the dynamic shear modulus, G, as 47MPa, and Poisson's ratio, μ, as 0.4, considering the recommendations from Bowles (1996).

Soil underneath each foundation is idealized as six springs to model stiffness corresponding to three translations and three rotations. The soil surrounding the building is modelled as translational springs at mid height of the basement columns. For the corner columns, two springs, i.e., in the X and Y-direction, were used; for the remaining columns only the out-of plane soil stiffness was taken into account. The soil interaction underneath the tie beams is idealized as translational springs along the two horizontal and vertical direction. Base, column and tie beam springs were modelled as SPRING1 elements in ABAQUS. The values of spring stiffness were calculated using the procedure proposed in Gazetas (1991). It is noted that this simple model does not take into account through-the-soil interaction between individual foundations present in some other formulations (Mulliken and Karabalis 1998). The equations and charts for calculating static and dynamic soil stiffness coefficients are based on length, L, width, B, base area, A, and second moments of area, I, of foundation, soil Poisson's ratio, μ, shear modulus and shear wave velocity, and dynamic response frequency, ω.

According to Gazetas' model, dynamic soil stiffness K_i for a particular degree of freedom i can be expressed as:

$$K_i = G \times f_i(\mu, L, B, A, I_i) \times k_i(\mu, L/B, \omega B/V_s) \qquad (2)$$

where $G \times f_i(\mu, L, B, A, I_i)$ is the static stiffness, and $k_i(\mu, L/B, \omega B/V_s)$ is the dynamic stiffness modification factor. Functions f_i and k_i are certain expressions of the parameters listed as their arguments. Superscript $i=1, 2, \ldots 6$ is applied to those functions and parameters that differ for different degrees of freedom. As can be seen,

in all cases stiffness is proportional to the shear modulus G. The dependence of static

stiffness on Poisson's ratio μ in functions f_i is more complex and varies between the

degrees of freedom. While not relevant for the numerical simulations discussed in this

section, later to vary soil stiffness during model updating, only the shear modulus was

changed. This was done in order to keep the number of updating parameters small and

simplify the calculation of sensitivities of natural frequencies to soil stiffness. The

dynamic stiffness modification factors k_i depend on the frequency of foundation

motion. A quick check of their values in the frequency range from 2.5Hz to 4.0Hz,

encompassing with some margin the full range of frequencies encountered in this

study when soil effects are considered, showed a very small maximum relative

variation of less than 1%. For this reason the frequency dependence of soil stiffness

was ignored and constant values corresponding to 3.04Hz (the lowest modal

frequency observed experimentally in Table 2) adopted.

Discussion of FEM results

The results of numerical modal analysis of different FEMs developed in Stages I-VI

are presented in Table 3 and compared to experimental results for the minimum

frequencies identified from the strongest seismic event available. Later, it is intended

to use an updated FEM for building serviceability limit state assessment that requires

it to be subjected to even stronger excitations and, in view of decreasing frequencies

with response levels, the minimum frequencies are more relevant. An important

observation from the analysis is that the values of frequencies of the bare frame, Stage

I, are significantly lower compared to the experimental ones, between 23.7% and

34.0%, and also those from the subsequent stages. This can be explained by the fact

that while practically all the mass is accounted for in Stage I important contributions

to stiffness from the shear core, NSCs and soil are not. Stage II adds slabs to the bare

17

frame, increasing the stiffness slightly to reduce the first, second and third modal frequency difference compared to the experimental results by 2.7%, 1.6% and 3.2%, respectively. Stage III incorporates the shear core which further reduces the first, second and third modal frequency difference by 7.5%, 23.1% and 17.0%, respectively, compared to the previous stage. By modelling NSCs in Stage IV, a further considerable increase can be observed in the frequencies from the previous Stage III: 17.9%, 22.4% and 19.3%. At this stage, the first frequency is slightly lower (2.0%) compared to the experimental value, while the second frequency is markedly higher (23.4%) and the third frequency is higher (5.5%) than their experimental counterparts. In Stage V, the fixed base was replaced by soil springs which caused a considerable decrease, 13.1%, 26.5% and 13.8% for the first, second and third modal frequency, respectively, from the previous Stage IV. The final Stage VI includes modelling of the soil surrounding the building in which case all the frequencies again increased, respectively by 10.8%, 10.6% and 14.1%. The above findings demonstrate that NSCs and SSI contribute significantly towards the modal dynamic response of the building, therefore, to replicate the true in-situ behaviour of the building these should not be ignored.

For the final FEM obtained in Stage VI, all the analytical frequencies are in a reasonable agreement with the measured values with all the errors not exceeding 7.5%. These differences can, however, be further reduced by tuning the final FEM developed in Stage VI using a sensitivity based model updating technique, a brief methodology of which and application to the FEM of the building are explained and discussed in the following section.

Sensitivity based model updating

Model updating is concerned with the calibration of the FEM of a structure such that it can better predict the measured responses of that structure. The sensitivity based model updating procedure generally comprises three steps: i) selection of reference experimental responses, ii) selection of model parameters to update, and iii) an iterative model tuning. In the sensitivity based updating, corrections and modifications are systematically applied to the local physical parameters of the FEM to modify them with respect to the experimental reference responses. The experimental responses are expressed as functions of the structural parameters and a sensitivity coefficient matrix in terms of a first order Taylor series (Brownjohn et al. 2001b) as:

$$R_e = R_a + S(P_u - P_0) \tag{3}$$

where R_e and R_a are the vectors of experimental and analytical response values, respectively, whereas P is the vector of model parameters, where subscripts u and 0 are for the updated and current values, respectively. Target, experimental responses R_e are usually the natural frequencies and mode shapes measured on the real structure, whereas updating parameters P are uncertain parameters in the FEM which can include geometric and material properties and boundary and connectivity conditions related to stiffness and inertia. S is the sensitivity matrix whose entries can be calculated as:

$$S_{ij} = \left. \frac{\partial R_{a,i}}{\partial P_j} \right|_{P=P_0} \tag{4}$$

Here $R_{a,i}$ $(i = 1, \ldots \ldots \ldots, n)$ and P_j $(j = 1, \ldots \ldots \ldots, m)$ are the entries of the analytical structural response and the updating structural parameter vectors, respectively. Equation (4) calculates absolute sensitivities expressed in the units of the response and parameter values. For comparing relative sensitivities of different types

of responses to relative changes in different parameters the normalized relative sensitivity matrix S_{nr} can be calculated as (Brownjohn et al. 2003):

$$S_{nr} = R_{D,a}^{-1} S P_D \qquad (5)$$

where $R_{D,a}$ and P_D are square, diagonal matrices holding analytical response and parameter values, respectively.

In this study, a Bayesian parameter estimation technique is used for updating the model with respect to the measured responses. This technique includes weighting coefficients applied to the updating parameters and experimental responses to accommodate the confidence levels in their estimation. The advantage of Bayesian estimation is better conditioning of the updating problem (Wu and Li 2004; FEMtools 2008). The difference between the experimental and model responses is resolved by using the following updating algorithm (Dascotte et al. 1995):

$$P_u = P_0 - G(R_e - R_a) \qquad (6)$$

where G is the gain matrix which can be computed as:

$$G = (C_a + S_{nr}^T C_e S_{nr})^{-1} S_{nr}^T C_e \qquad (7)$$

$$G = C_a^{-1} S_{nr}^T (C_e^{-1} + S_{nr} C_a^{-1} S_{nr}^T)^{-1} \qquad (8)$$

Equation (7) is valid for the case when the number of responses is not less than the number of updating parameters, whereas Equation (8) is used in the case of fewer responses than the updating parameters. Here, C_e and C_a represent diagonal weighting matrices expressing the confidence in the values of experimental and model responses, respectively, and superscript T denotes matrix transpose.

The important considerations regarding parameter selection for updating are the number of parameters to be updated and preference of certain parameters among many possible candidates. An excessive number of parameters compared to the number of available responses, or overparametrisation, will lead to a non-unique

solution, whereas insufficient number of parameters will prevent reaching a good agreement between the experiment and model (Titurus and Friswell 2008). The selected parameters should be uncertain and expected to vary within certain bounds, otherwise updating may result in physically meaningless results. If there are a number of candidate parameters available for updating, sensitivity analysis using the normalized relative sensitivities (Equation (5)) can help to retain only those parameters that significantly influence the responses.

Calibration of the FEM of the instrumented building

The objective of this part of the study is to calibrate the FEM to replicate the true behaviour of the instrumented building under the largest of the selected 50 earthquakes. The reason for using the maximum recorded earthquake is to obtain a representative model of the structure, whose properties have been shown in this study to be amplitude dependent, to be later used for time history analyses under scaled-up excitations minimizing as much as possible extrapolation of the model to those levels of shaking. The presentation comprises comparison between FEM and experimental responses, sensitivity analysis and selection of responses and updating parameters, and, finally, discussion of updated results.

Comparison between initial FEM and experimental results

For this study, FEM results are compared and calibrated with the dynamic properties of the flexible base model identified during the largest recorded earthquake (in terms of PGAs and PRAs measured at the site) of October 10th, 2009, which had an epicentre 20km North-West of Wellington, moment magnitude M_W=4.8, PGA at the free field and base of 0.0138g and 0.0093g, respectively, and PRA of 0.0412g in the more strongly excited Y-direction (see Table 1). The identified first three modal

frequencies (Table 4) during this event were 3.04Hz, 3.21Hz and 3.48Hz,

respectively, whereas the corresponding damping ratios were 4.7%, 4.6% and 3.6%

respectively. The final Stage VI FEM developed in ABAQUS was imported into

FEMtools software (FEMtools 2008) for performing model updating. (Note FEMtools

calculated slightly different first three frequencies compared to ABAQUS as can be

seen in Tables 3 and 4).

A comparison between dynamic properties of the FEM and measured

responses is presented in Table 4. Table 4 shows that the relative errors between the

individual initial FEM and measured frequencies are under 7.5% for all three modes.

The correlation of mode shapes is expressed using model assurance criterion (MAC)

values. For mode shapes $\boldsymbol{\phi}_i$ and $\boldsymbol{\phi}_j$, MAC is defined as (Ewins 2000):

$$MAC = \frac{\left(\boldsymbol{\phi}_i^T \boldsymbol{\phi}_j\right)^2}{\left(\boldsymbol{\phi}_i^T \boldsymbol{\phi}_i\right)\left(\boldsymbol{\phi}_j^T \boldsymbol{\phi}_j\right)} \times 100\% \tag{9}$$

The similarity of mode shapes is very good, 92%, for the second mode, while for the

first and third modes MAC values are reasonably satisfactory, being 78% and 63%,

respectively. The MAC matrix illustrating orthogonality conditions between all

combinations of the initial FEM and measured mode shapes is shown in Figure 5a. In

this figure, the large diagonal values are the same as reported in Table 4, and the

much lower off-diagonal values confirm the correct pairing of experimental and

numerical mode shapes. It is noted, however, that MAC between the second FEM and

third experimental mode is noticeably high.

Sensitivity analysis and selection of response and updating parameters

The updating process starts with identifying target responses and model parameters to

update. In this study the measured first three natural frequencies were taken as target

responses to be replicated by the model. It was assumed that the identified frequencies

used as targets have a scatter of 2%. Since there was not enough frequencies with the amplitude of response similar to the record used for model updating, the scatter was estimated using the frequencies identified for X-direction PRAs between 0.0008998g and 0.0009869g where there was enough data for very similar PRAs and not affected by the observed frequency-PRA trends (see Figure 4a). Therefore, this confidence level was applied to the target responses to define any uncertainty in the experimental data as the diagonal weighting matrix C_e entries (Equations (7) and (8)).

The updating parameters were selected based on their expected uncertainty and the sensitivity analysis to determine the most influential parameters to produce a genuine improvement in the model. Only stiffness parameters were considered for updating as mass can normally be determined with less uncertainty. Three parameters, namely: i) shear modulus of soil, ii) modulus of elasticity of the cladding, and iii) modulus of elasticity of concrete were finally selected. The normalized relative sensitivities of the target responses to the parameters are shown in Table 5. It can be observed from the table that the values of the normalized relative sensitivities S_{nr} considering all the responses show a significant sensitivity for producing a change in the response. Modulus of elasticity of concrete is the most influential parameter while the remaining two are almost equally influential but roughly 50% less than the first. Confidence levels were applied to the updating parameters as the diagonal weighting matrix C_a entries (Equations (7) and (8)) to take into account uncertainty in their estimation. For this study, it is assumed that the updating parameters can have a scatter within ±30%.

Updating results and discussions

FEMtools software (FEMtools 2008) was used in this research for automatic model updating. In the model updating procedure, error interpreted as an objective function

23

is minimized to improve the response prediction of the model. The following objective function, representing mean weighted absolute relative frequency error, is considered in this study:

$$e_f = \frac{1}{n} \sum_{i=1}^{n} c_{ri} \frac{|\Delta f_i|}{f_i} \times 100\% \tag{10}$$

where n is the total number of target frequencies considered, and f_i and Δf_i are the target frequency and frequency error, respectively, whereas coefficients c_{ri} account for the estimated relative variabilities of responses.

The automatic iterative procedure for minimizing the objective function is controlled by a following three convergence criteria:

   i)   the minimum value of objective function, assumed 0.1%;

   ii)   the minimum improvement in the objective function between two consecutive iterations, assumed 0.01%; and

   iii)   the maximum number of iterations allowed, assumed 50.

The algorithm searching for the global minimum of the objective function may be lured into local minima instead of the global minimum in problems that Goldberg et al. (1992) call 'deceptive'. This undesirable behaviour is well known in the context of model updating using sensitivity method (Deb 1998). In this study, a two-step updating strategy was followed to safeguard against being trapped in a local minimum (Brownjohn and Xia 2000):

• Step 1: Starting with the initially assumed values of updating parameters the objective function is minimized to arrive at an intermediate solution; and

• Step 2: The values of the updated parameters obtained in Step 1 were perturbed by +10%, 0% and -10%, considering all 27 combinations, and the updating procedure rerun.

Results of updating are shown in Table 4. In Step 1, the objective function, e_f, has improved considerably from 6.11% to 0.31%, with the largest individual error not exceeding 0.33%. While MACs were not explicitly included in the objective function, improving frequencies typically also improves MACs. This was also the case in the reported exercise: the MAC values have improved slightly for the first and second mode and are now equal to 80% and 96%, respectively, while for the third mode shape it has improved considerably reaching 79%. Table 6 shows the initial and updated values of stiffness parameters and their relative changes. It can be seen that the reported changes in modal characteristics were achieved by changing the stiffness of cladding by -38.1% and 21.7% for concrete, respectively. The soils stiffness practically did not change (-0.04%).

Due to space limitations, individual results from the 27 runs in Step 2 are not shown here, however, four clusters of points were discernible. A better solution to that of Step 1 was found among them, suggesting that Step 1 solution was only a local minimum and confirming the advantage and need of using the two-step procedure. Step 2 converged to a very small value of e_f=0.03% for the objective function, providing excellent match of frequencies with the maximum absolute error of 0.07% (see Table 4), and yielding the final updating parameter values of 42.3MPa for shear modulus of soil, 6.5GPa for modulus of elasticity of cladding, and 38.4GPa for modulus of elasticity of concrete (see Table 6). Compared to the initial values the relative changes were -10.0%, -35.1% and 27.8%, respectively. The shifts in relative values compared to Step 1 were smaller for cladding and concrete, -3.7% and 6.1%, and more noticeable, -10.0%, for soil.

Step 2 practically did not change the MACs and their final values are 80%, 96% and 78%. However, improvements in MACs compared to the initial FEM are

noticeable. The updated MAC matrix is shown graphically in Figure 5b. The reduction in the height of the off-diagonal terms is also clear in the figure. Figure 6 shows the comparison between the measured and updated FEM mode shapes at the roof level assuming the roof to act like a rigid diaphragm. It can be observed from Figure 6 that the second mode shapes coincide very well, while the first and third mode shapes are matched reasonably well.

No updating exercise is complete without assessing the plausibility of numerically obtained results and clear understanding of their limitations. The large drop in the cladding stiffness (-35.1%) indicates that the assumption of the cladding being fully fixed to the structural elements was not justified and very likely only partial fixity exists. Another reason for reduced stiffness are the openings for windows in the cladding panels which were ignored in the FEM model. Also an initial overestimation of cladding material modulus of elasticity, taken from literature, is quite possible. For the modulus of elasticity of concrete the increase is by 27.8%. The increased value is not outside the typically encountered significant variability of concrete properties. Also, the initial estimate of modulus of elasticity of RC was based on typical, conservatively assumed values used in New Zealand building construction of the era but the exact design or laboratory tested values were unknown. For those reasons, the updated value is not unreasonable. It is also possible that other non-structural elements, whose stiffness was not updated, could have made a contribution towards larger stiffness. One would expect more uncertainty in the soils properties, but, perhaps unexpectedly, the change in the soil shear modulus after updating was only -10.0%. This was rather due to luck in the initial estimate than anything else. For all the parameters it needs to be emphasized that they are the global stiffness of soil, concrete and cladding without taking into account any possible local

spatial variations. In general, the updated model represents the optimal solution for the frequency matching problem of Equation (10) that is also justified by engineering judgment, but hinges on the validity of the initial model topology, discretization and parameterization. We argue though that these are adequate.

Validation of the updated model

To further validate the updated FEM, the simulated response is compared with the recorded response of the earthquake of October 10th, 2009, that produced the largest PGAs and PRAs at the building site. The updated FEM was exported to ABAQUS from FEMtools to perform time history analysis. For time history analysis, all three directions of the acceleration record measured at the base level at sensor 6 were applied simultaneously at all the column foundations in agreement with the fact that there are tie-beams linking all the foundations and that the measured accelerations at the base level at sensor 6 and 7 were the same for practical reasons. A constant damping of 5% was considered for all the modes as recommended by NZS 1170.5 (Standards New Zealand 2004) for time history analysis for serviceability limit state. (This code recommended damping ratio was used rather than the identified values due to considerable spread of the latter as mentioned earlier. Table 4 shows that the measured values were not significantly different than 5% either.)

To quantify the improvement in response prediction due to updating the following relative error measures were adopted (Sprague and Geers 2004):

$$e_{mag} = \sqrt{\frac{\sum_{t=1}^{N} a_s^2(t)}{\sum_{t=1}^{N} a_m^2(t)}} - 1 \qquad (11)$$

$$e_{\theta} = \frac{1}{\pi} \cos^{-1}\left(\frac{\sum_{t=1}^{N} a_s(t)a_m(t)}{\sqrt{\sum_{t=1}^{N} a_s^2(t) \sum_{t=1}^{N} a_m^2(t)}}\right) \qquad (12)$$

where e_{mag} and e_θ are, respectively, the relative errors in the magnitude and phase between the simulated, $a_s(t)$, and measured, $a_m(t)$, acceleration time histories, $t=1, 2,$ … N is the discrete time, and N is the total number of time steps. The magnitude error e_{mag} is not influenced by time shifts between two signals. This metric has also another advantage of being able to take a positive or negative sign showing which of the two records has a larger mean magnitude. The phase error e_θ is, on the other hand, influenced by time shifts between two signals but not their relative magnitudes. The reason for using these error metrics, instead of, for example, sometimes employed root mean square of the time history of the difference between the simulated and measured responses, is that the latter is sensitive to time shifts between the two time histories resulting in a large error for what is correctly perceived as quite similar time histories and a rather meaningless comparison (Schwer 2007).

Table 7 shows the summary of error measures e_{mag} and e_θ. Figures 7a-c show the comparison between actual recorded and simulated responses of initial and updated FEMs in the form of acceleration time histories at representative locations (sensor 3 at the roof for both horizontal directions; and sensors 3 and 4 at the roof for torsion). Torsional acceleration is calculated as the difference between the X-direction acceleration records of sensors 3 and 4 divided by the distance between them. It can be observed from Table 7 that e_{mag} in translational response along X-direction has improved from -0.13 to 0.06, for Y-direction response from -0.36 to -0.26, whereas for torsion from -0.17 to -0.09. On the other hand, the improvement in e_θ for X-direction is from 0.33rad to 0.18rad, for Y-direction from 0.34rad to 0.28rad, and for torsional direction from 0.41rad to 0.30rad. From the point of view of the building seismic performance, phase can be considered relatively less important than magnitude. From the magnitude errors after updating it can be concluded that the

28

agreement of simulated and measured responses along X- and torsional directions has improved markedly and is now very close, whereas along Y-direction, despite some improvement, more noticeable difference is still present. The phase errors also decreased and are now between 0.18rad and 0.30rad.

Assessment of serviceability limit state performance using initial and updated FEM

Under the serviceability limit state, the building response should remain predominantly elastic and avoidance of excessive lateral deformations to prevent non-structural damage is the primary control parameter. The inter-story drift ratio, defined as the relative displacement between the top and bottom of the story divided by story height, is commonly assumed to control the onset of non-structural damage (Dymiotis-Wellington and Vlachaki 2004). Therefore, to study the serviceability limit state performance of the building, the maximum inter-story drift ratios for a random selection of 10 seismic events recorded at the building site (see Table 8) and appropriately scaled were calculated. For the purpose of comparison, the analysis is performed for both the initial and updated FEMs.

All the available earthquakes recorded at the building site are of low intensity, it is therefore necessary to scale those to the serviceability limit state level shaking. The scaling procedure recommended in the NZS 1170.5 (Standards New Zealand 2004) was followed for the selected 10 earthquakes. In short, it requires minimizing the logarithmic root-mean-square difference between the actual and target spectra in a frequency range encompassing the fundamental frequency of the structure at hand. The assumed target code spectrum for a return period of 25 years and hazard factor of 0.4 is shown in Figures 8a and b along with the spectra of the 10 earthquakes for both X- and Y-direction components, respectively. The scaling factors for the selected 10

29

events to match the target spectrum are reported in Table 8; they range between 17 and 676. Since the measured X- and Y- components of the records were different, the scaling factors for both orthogonal components are also different. The period range for spectrum matching was between 0.13sec and 0.43sec (2.32Hz and 7.69Hz).

For calculating inter-story drift ratios, the scaled X- and Y-direction components of a record were applied simultaneously to run the time history analysis for both initial and updated FEMs. As previously, when validating the updated FEM, a constant damping of 5% was considered for all the modes. The lateral displacements along X- and Y-directions at the four corners of each floor level were determined, inter-story drift ratios corresponding to the two directions calculated separately, and maximum ratios selected. For all the considered excitation cases, the largest inter-story drift ratios were observed between the first and the ground floor. Table 8 shows the maximum inter-story drift ratios for the considered 10 earthquakes for both initial and updated FEMs along X- and Y-directions. The values for X-direction are between 0.06% and 0.16% and between 0.07% and 0.21% for the initial and updated model, respectively; for Y-direction these ranges are between 0.06% and 0.13% and between 0.07% and 0.15%, respectively. It can be observed that the updated FEM provides larger inter-story drift ratios, by 31% and 25% for the X- and Y-direction, respectively, than the initial FEM. This is because it is less stiff as evident from the modal frequencies, however, since the relative increase varies between the earthquakes matching of building resonant frequencies and spectral content of excitation play a role too.

The recommended limiting inter-story drift ratios reported in the literature and recommended by various codes vary widely between 0.06% and 0.6% (Bertero et al. 1991). Dymiotis-Wellington and Vlachaki (2004) recommend 0.2% as the critical

inter-story drift ratio based on their observations on RC buildings. They argued that higher limiting values can cause significant yielding in the structure and correspond to a damage state beyond serviceability. Taking this latter limit value, it can be concluded that for the considered scaled seismic events, the building has reached or just exceeded the serviceability limit state of 0.2% inter-story drift for two events, EQ1 and EQ8, for the updated FEM (Table 8). Overall, the serviceability performance can be judged as satisfactory. However, the initial FEM produced unconservative, lower values. This confirms the benefit and importance of using a calibrated structural model in checking performance criteria.

Finally, since linear FEMs were used in the serviceability study, it is in order to assess if the linearity assumption is justified. The maximum inter-story drift ratio reported in Table 8 is 0.21%, with the majority of values noticeably lower. Insufficient information is available (such as the exact reinforcement ratios and detailing, or on nonlinear behaviour of cladding and its connections to the RC frame) that would enable the creation of a detailed and realistic nonlinear FEM to be subjected to time history analysis to see if it enters nonlinear range at the serviceability level response. However, some indirect inferences can be made. Serviceability limit state can be understood as separating the linear and nonlinear structural behaviour (Dymiotis-Wellington and Vlachaki 2004). Mosalam et al. (1997) considers it to be limited to the case of insignificant damage where repair is only required to non-structural elements, and gives the critical inter-story drift ratio in the range between 0.2% and 0.5%. Eurocode 8 (European Committee for Standardisation (2003) also implies avoidance of damage and gives similar limits for the inter-storey drift ratios for damage in non-structural elements between 0.2% and 0.5%. As far as yielding in structural elements is concerned, a study by Dymiotis-

Wellington and Vlachaki (2004) showed, despite its limited scope, that inter-story drifts of 0.2% resulted in mild yielding (rotational ductility less than 2) in only some beams of an RC frame designed to Eurocode 8. As in our study the maximum inter-story drift ratio is 0.21%, with the majority of remaining values noticeably lower, there are good reasons to believe that the building will experience at most only mild nonlinear responses and the linear FEM used were able to predict its serviceability limit state behaviour reasonably well.

Conclusions

This study was concerned with seismic response of an instrumented three story RC building. The first part focused on review of modal properties identified using 50 seismic response records. The records, varying in amplitude, enabled determination of trends in frequencies with increasing amplitude of response. The frequencies showed a clear decreasing trend with increasing PRA, which could be reasonably represented by a linear relationship. The identified damping ratios, however, had scattered values with no clear trend.

The second part was concerned with numerical modelling of the building and its seismic responses. As series of FEMs including SSI and NSCs was first developed and the influence of different structural and non-structural components, and the effect of soil on the building dynamics analysed. It was found that NSCs and SSI contribute significantly to modal dynamic response and these should be included in FEMs to replicate the true in-situ behaviour. The final FEM produced resonance frequencies within 7.5% of those identified experimentally. The final FEM was further improved using a sensitivity based model updating technique. The updating parameters included a structural parameter (stiffness of concrete), a non-structural parameter (stiffness of cladding), and soil stiffness. The match between the frequencies after updating was

32

found to be very good (within 0.07%), while the agreement in mode shapes was also improved. The updated FEM was then further validated by examining how well it replicated the recorded acceleration time histories. The updated FEM has significantly improved the predictions of response magnitude and reduced errors in phase predictions.

Finally, the updated FEM was used to study the seismic structural performance of the building at the serviceability limit state shaking. The maximum inter-story drift ratios were calculated for a selection of 10 scaled earthquakes recorded at the building site. It was found that the updated FEM produced larger drifts as compared to the initial FEM. For the updated FEM, the inter-story drift ratios reached in some cases the recommended critical values, but the overall building serviceability limit state performance was judged as satisfactory.

Acknowledgements

References

ABAQUS (2011). ABAQUS theory manual and user's manual. Providence, R.I, Dassault Systemes Simulia Corporation.

ASCE/SEI 7-05 (2005). Minimum design loads for buildings and other structures. Reston, VA, Structural Engineering Institute of the American Society of Civil Engineers.

Bertero, V. V., Anderson, J. C., Krawinkler, H., Miranda, E. and the CURE and Kajima Research Teams (1991). Design guidelines for ductility and drift limits: Review of state-of-the-art in ductility and drift-based earthquake resistant design of buildings. UCB/EERC 91/15, Berkeley, CA, The University of California.

Berto, L. R., Vitaliani, A., Saetta, A. and Simioni, P. (2009). "Seismic assessment of existing RC structures affected by degradation phenomena." Structural Safety 31(4): 284-297.

Bhattacharya, K. and Dutta, S. C. (2004). "Assessing lateral period of building frames incorporating soil flexibility." Journal of Sound and Vibration 269(3-5): 795-821.

Bodeux, J. B. and Golinval, J. C. (2001). "Application of ARMAV models to the identification and damage detection of mechanical and civil engineering structures." Smart Materials and Structures, 10: 479-489.

Boon, D., Perrin, N. D., Dellow, G. D., Van Dissen, R. and Lukovic, B. (2011). "NZS1170.5:2004 site subsoil classification of Lower Hutt." Proceedings of the 2011 Pacific Conference on Earthquake Engineering, Auckland: 1-8.

Bowles, J. E. (1996). Foundation analysis and design. Singapore, McGraw-Hill.

Brownjohn, J. M. W., Hong, H. and Chien, P. T. (2001a). Assessment of structural condition of bridges by dynamic measurements. Singapore, Nanyang Technological University.

Brownjohn, J. M. W., Moyo, P., Omenzetter, P., and Lu, Y. (2003). "Assessment of highway bridge upgrading by dynamic testing and finite-element model updating." Journal of Bridge Engineering, ASCE 8(3): 162-172.

Brownjohn, J. M. W. and Xia, P. Q. (2000). "Dynamic assessment of curved cable-stayed bridge by model updating." Journal of Structural Engineering, ASCE 126(2): 252-260.

Brownjohn, J. M. W., Xia, P. Q., Hao, H., and Xia, Y. (2001b). "Civil structure condition assessment by FE model updating: Methodology and case studies." Finite Elements in Analysis and Design 37(10): 761-775.

Butt, F. and Omenzetter, P. (2012)."Evaluation of seismic response trends from long-term monitoring of two instrumented RC buildings including soil-structure interaction." Advances in Civil Engineering 2012:1-18.

Celebi, M. (2006). "Recorded earthquake responses from the integrated seismic monitoring network of the Atwood building, Anchorage, Alaska." Earthquake Spectra 22(4): 847-864.

Celebi, M. and Safak, E. (1991). "Seismic response of Transamerica building. I: Data and preliminary analysis." Journal of Structural Engineering, ASCE 117(8): 2389-2404.

Celebi, M. and Safak, E. (1992). "Seismic response of Pacific Park Plaza. I: Data and preliminary analysis." Journal of Structural Engineering, ASCE 118(6): 1547-1565.

European Committee for Standardisation (2003). Eurocode 8: Design of structures for earthquake resistance - Part 1: General rules, seismic actions and rules for buildings. Brussels, European Committee for Standardisation.

Dascotte, E., Strobbe, J. and Hua, H. (1995). "Sensitivity based model updating using multiple types of simultaneous state variables." Proceedings of the 13th International Modal Analysis Conference. Bethel, MN: 1-6.

Deb, K. (1998). Optimization for engineering design: algorithms and examples. New Delhi, Prentice-Hall of India.

Dymiotis-Wellington, C. and Vlachaki, C. (2004). "Serviceability limit state criteria for the seismic assessment of RC buildings." Proceedings of the 13th World Conference on Earthquake Engineering. Vancouver, BC: 1-10.

Ewins, D. J. (2000). Modal testing: Theory, practice and application. Baldock, Research Studies Press.

FEMtools (2008). FEMtools model updating theoretical manual and user's manual. Leuven, Dynamic Design Solutions.

Foti, D., Diaferio, M., Giannoccaro, N. I. and Mongelli, M. (2012). "Ambient vibration testing, dynamic identification and model updating of a historic tower." Nondestructive Testing and Evaluation International 47: 88-95.

Friswell, M. I. and Mottershead, J. E. (1996). Finite element model updating in structural dynamics. Dordrecht, Netherlands, Kluwer Academic Publishers.

Gaylord, M. W. (1974). Reinforced plastics: Theory and practice. New York, NY, Cahners.

Gazetas, G. (1991). "Formulas and charts for impedances of surface and embedded foundations." Journal of Geotechnical Engineering, ASCE 117(9): 1363-1381.

GeoNet (2013). Structural array data. http://info.geonet.org.nz/display/appdata/Structural+Array+Data, accessed 30 July 2013.

Geers, T. L. (1984). "An objective error measure for the comparison of calculated and measured transient response histories." The Shock and Vibration Bulletin 54(2): 99-107.

Goldberg, D. E., Deb, K. and Horn, J. (1992). Massive multimodality, deception, and genetic algorithms, Parallel Problem Solving from Nature 2: 37-46.

Hart, G. C. and Yao, J. T. P. (1976). "System identification in structural dynamics." Journal of Engineering Mechanics, ASCE 103(6): 1089–1104.

Kanvinde, A. M., and Deierlein, G. G. (2006). "Analytical models for the seismic performance of gypsum drywall partitions." Earthquake Spectra 22(2): 391-411.

Lee, T. H., Kato, M., Matsumiya, T., Suita, K. and Nakashima, M. (2007). "Seismic performance evaluation of non-structural components: Drywall partitions." Earthquake Engineering and Structural Dynamics 36(3): 367-382.

Lin, C. C., Wang, J. F. and Tsai, C. H. (2008). "Dynamic parameter identification for irregular buildings considering soil-structure interaction effects." Earthquake Spectra 24(3): 641-666.

Montgomery, D., Peck, E. A. and Vining, G. (2001). Introduction to linear regression analysis. New York, NY, Wiley.

Mosalam K. M., Ayala G., White R. N. and Roth C. (1997). "Seismic reliability of LRC frames with and without masonry infill walls." Journal of Earthquake Engineering, ASCE, 1(4): 693-720.

Mulliken, J. S. and Karabalis, D. L. (1998). "Discrete model for dynamic through-the-soil coupling of 3-D foundations and structures." Earthquake Engineering and Structural Dynamics 27(7): 687-710.

Pan, T. C., You, X. and Brownjohn, J. M. W. (2006). "Effects of infill walls and floor diaphragms on the dynamic characteristics of a narrow-rectangle building." Earthquake Engineering and Structural Dynamics 35(5): 637-651.

Safak, E. (1993). "Response of a 42-storey steel-frame building to the M_S=7.1 Loma Prieta earthquake." Engineering Structures 15(6): 403-421.

Saito, T. and Yokota, H. (1996). "Evaluation of dynamic characteristics of high-rise buildings using system identification techniques." Journal of Wind Engineering and Industrial Aerodynamics 59(2-3): 299-307.

Satake, N. and Yokota, H. (1996). "Evaluation of vibration properties of high-rise steel buildings using data of vibration tests and earthquake observations." Journal of Wind Engineering and Industrial Aerodynamics 59(2-3): 265-282.

Schwer, L. E. (2007). "Validation metrics for response histories: Perspectives and case studies." Engineering with Computers 23: 295-309.

Shakib, H. and Fuladgar, A. (2004). "Dynamic soil-structure interaction effects on the seismic response of asymmetric buildings." Soil Dynamics and Earthquake Engineering 24(5): 379-388.

Sohn, H., Farrar, C. R., Hemez, F. M., Shunk, D. D., Stinemates, D. W. and Nadler, B. R. (2003). A review of structural health monitoring literature: 1996–2001. Los Alamos, NM, Los Alamos National Laboratory.

Sprague, M. A. and Geers, T. L. (2004). "A spectral-element method for modelling cavitation in transient fluid-structure interaction." International Journal for Numerical Methods in Engineering 60(15): 2467-2499.

Standards New Zealand (2004). NZS 1170.5:2004. Structural design actions. Part 5: Earthquake actions – New Zealand. Wellington, Standards New Zealand.

Steel, R. and Torrie, J. (1960). Principles and procedures of statistics. New York, NY, McGraw-Hill.

Stewart, J. P. and Fenves, G. L. (1998). "System identification for evaluating soil-structure interaction effects in buildings from strong motion recordings." Earthquake Engineering and Structural Dynamics 27(8): 869-885.

Su, R. K. L., Chandler, A. M., Sheikh, M. N. and Lam, N. T. K. (2005). "Influence of non-structural components on lateral stiffness of tall buildings." Structural Design of Tall and Special Buildings 14(2): 143-164.

Titurus, B. and Friswell, M. I. (2008). "Regularization in model updating." International Journal for Numerical Methods in Engineering 75: 440-478.

Trifunac, M. D., Ivanovic, S. S. and Todorovska, M. I. (2001). "Apparent periods of a building. I: Fourier analysis." Journal of Structural Engineering, ASCE 127(5): 517-526.

Trifunac, M. D. and Todorovska, M. I. (1999). "Recording and interpreting earthquake response of full-scale structures." Proceedings of the NATO Advanced Research Workshop on Strong-Motion Instrumentation for Civil Engineering Structures. Dordrecht, Kluwer: 131-155.

Uma, S. R., Zhao, J. X. and King, A. B. (2010). "Seismic actions on acceleration sensitive non-structural components in ductile frames." Bulletin of the New Zealand Society for Earthquake Engineering 43(2): 110-125.

Van Overschee, P. and De Moor, B. (1994). "N4SID: Subspace algorithms for the identification of combined deterministic-stochastic systems." Automatica 30(1): 75-93.

Wang, H., Li, A. and Li, J. (2010). "Progressive finite element model calibration of a long-span suspension bridge based on ambient vibration and static measurements." Engineering Structures 32(9): 2546-2556.

Weng, J.-H., Loh, C.-H. and Yang, J. N. (2009). "Experimental study of damage detection by data-driven subspace identification and finite element model updating." Journal of Structural Engineering, ASCE 135(12): 1533-1544.

Wu, J. R. and Li, Q. S. (2004). "Finite element model updating for a high-rise structure based on ambient vibration measurements." Engineering Structures 26(7): 979-990.

Zhang, Q. W., Chang, C. C. and Chang, T. Y. P. (2000). "Finite element model updating for structures with parametric constraints." Earthquake Engineering and Structural Dynamics, 29(7): 927-944.

Table 1. Maximum PGA and PRA recorded by individual sensors.

Sensor	Max. acceleration in X-direction (g)	Max. acceleration in Y-direction (g)
Free field		
10 (PGA)	0.0074	0.0138
Foundation		
6 (PGA)	0.0059	0.0092
7 (PGA)	0.0061	0.0090
Roof		
3 (PRA)	0.0185	0.0390
4 (PRA)	0.0206	0.0412

Table 2. Summary of identified frequencies and damping ratios for flexible base model.

Mode	Frequency				Damping ratio			
	Min. (Hz)	Max. (Hz)	Avg. (Hz)	Relative spread (%)	Min. (%)	Max. (%)	Avg. (%)	Relative spread (%)
1st	3.04	3.50	3.33	14	1.2	7.3	3.4	176
2nd	3.21	3.88	3.61	19	1.4	12.1	5.6	190
3rd	3.48	3.90	3.79	11	1.0	8.3	3.1	240

Butt and Omenzetter

Table 3. Comparison of results of different stages of FEM modal analysis with measured values.

Mode	Frequencies (Hz)						
	Stage I	Stage II	Stage III	Stage IV	Stage V	Stage VI	Measured value
1st	2.12 (-30.3%)	2.20 (-27.6%)	2.43 (-20.1%)	2.98 (-2.0%)	2.58 (-15.1%)	2.91 (-4.3%)	3.04
2nd	2.45 (-23.7%)	2.50 (-22.1%)	3.24 (1.0%)	3.96 (23.4%)	3.11 (-3.1%)	3.45 (7.5%)	3.21
3rd	2.30 (-34.0%)	2.41 (-30.8%)	3.00 (-13.8%)	3.67 (5.5%)	3.19 (-8.3%)	3.68 (5.8%)	3.48

Note: The values in parenthesis show the percentage difference between the particular FEM stage and measured values.

Butt and Omenzetter

Table 4. Correlation between initial and updated FEMs and measured response of October 10th, 2009.

Mode	Measured responses		FEM frequencies (Hz)			Difference between FEM and measured frequencies (%)			MAC (%)		
	Frequency (Hz)	Damping ratio (%)	Initial model	Updating Step 1	Updating Step 2	Initial model	Updating Step 1	Updating Step 2	Initial model	Updating Step 1	Updating Step 2
1st	3.04	4.7	2.92	3.03	3.038	-3.95	-0.33	-0.07	78	80	80
2nd	3.21	4.6	3.45	3.20	3.21	7.48	-0.31	0.00	92	96	96
3rd	3.48	3.6	3.72	3.49	3.479	6.90	0.29	-0.03	63	79	78
Objective function e_f						6.11	0.31	0.03			

Butt and Omenzetter

Table 5. Normalized relative sensitivities of responses to updating parameters.

Updating parameter Response	Shear modulus of soil	Modulus of elasticity of cladding	Modulus of elasticity of concrete
1st modal frequency	0.12	0.13	0.24
2nd modal frequency	0.15	0.06	0.22
3rd modal frequency	0.11	0.10	0.25

Butt and Omenzetter

Table 6. Changes in the updating parameters.

Parameter	Initial value	Updating Step 1		Updating Step 2	
		Updated value	Relative change from initial value	Updated value	Relative change from initial value
Shear modulus of soil	47MPa	46.98MPa	-0.04%	42.3MPa	-10.0%
Modulus of elasticity of cladding	10.0GPa	6.8GPa	-31.8%	6.5GPa	-35.1%
Modulus of elasticity of concrete	30GPa	36.5GPa	21.7%	38.4GPa	27.8%

Table 7. Magnitude and phase errors in response time histories for initial and updated models

Direction	X		Y		Torsional	
FEM	Initial	Updated	Initial	Updated	Initial	Updated
e_{mag} (-)	-0.13	0.06	-0.36	-0.26	-0.17	-0.09
e_θ (rad)	0.33	0.18	0.34	0.28	0.41	0.30

Butt and Omenzetter

Table 8. Earthquake records used in serviceability study, scaling factors and maximum inter-story drift ratios

Earthquake designation	Date (DD/MM/YYYY) and time of occurrence (GMT)	PGA recorded at sensor 6 (g)		Scaling factor		Maximum inte	
		X-direction	Y-direction	X-direction	Y-direction	X-direction	
						Initial FEM	U F
EQ1	09/06/2008, 02:58	0.0016	0.0013	74	82	0.12	0
EQ2	09/14/2008, 09:25	0.0014	0.0018	81	65	0.13	0
EQ3	10/17/2008, 00:25	0.0003	0.0004	676	443	0.10	0
EQ4	12/26/2008, 19:49	0.0032	0.0032	35	33	0.06	0
EQ5	05/01/2009, 05:16	0.0036	0.0022	52	64	0.09	0
EQ6	08/05/2009, 17:51	0.0010	0.0016	123	71	0.07	0
EQ7	10/10/2009, 05:02	0.0059	0.0092	22	17	0.09	0
EQ8	11/18/2009, 1804	0.0022	0.0025	41	42	0.16	0
EQ9	12/08/2009, 22:09	0.0018	0.0018	78	67	0.07	0
EQ10	02/12/2010, 13:41	0.0034	0.0029	34	41	0.08	0

Butt and Omenzetter

Stairs   Elevator shaft

6.86m

5.33m

N

X

Y

11 x 4.064 m = 44.70m

a)

Sensor 4   Elevator shaft   Sensor 3

Third floor 13.40m

Second floor 9.90m

First floor 6.40m

Ground floor 2.90m

Basement 0.00m

Sensor 5

Sensor 7

Sensor 6

Vertical

X

Y

39.40m

1.80m

Sensor 10 (free field)
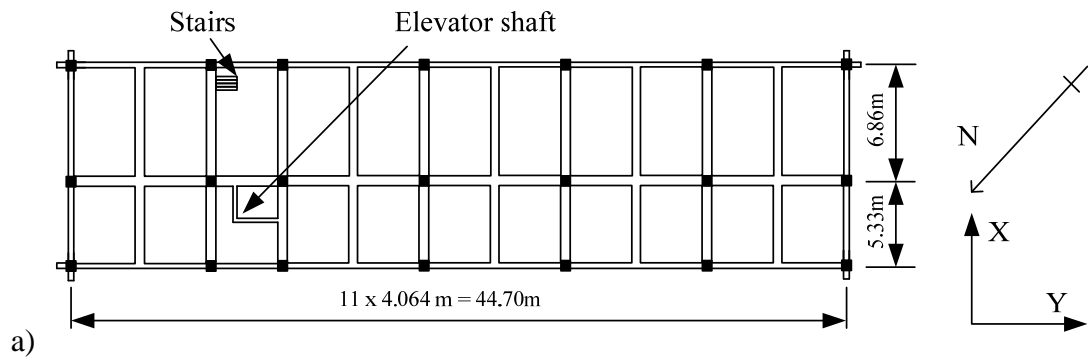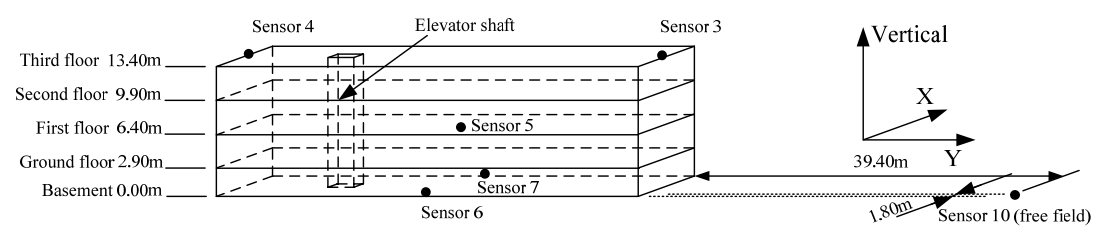
b)

Figure 1. Instrumented RC building: a) typical floor plan showing general dimensions and location of stairs and elevator shaft, and b) 3D view of the building and sensor array.
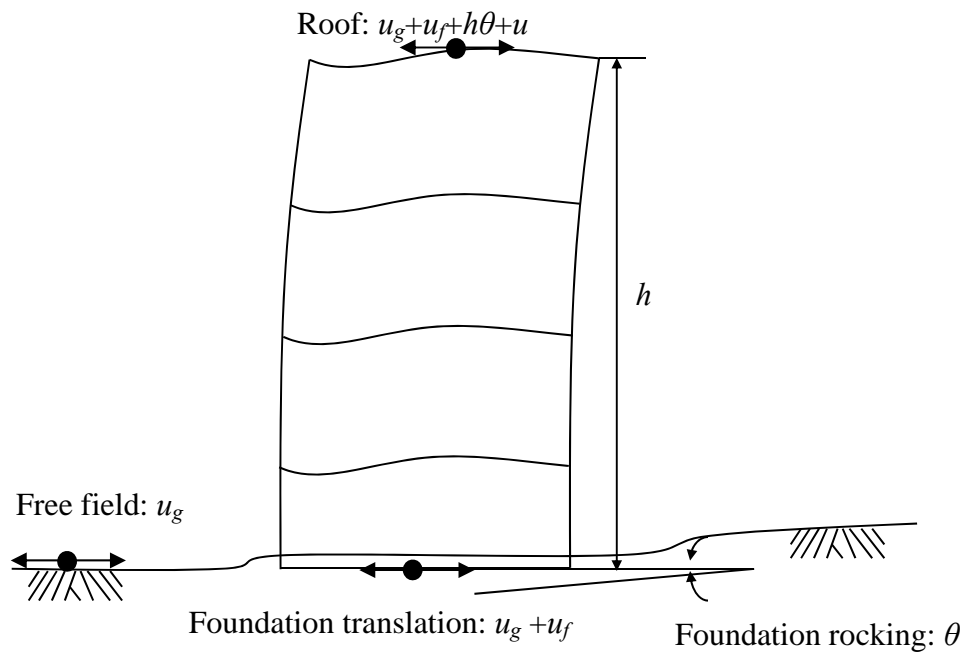
Butt and Omenzetter

1

Roof: $u_g+u_f+h\theta+u$

Free field: u_g

h

Foundation translation: $u_g +u_f$

Foundation rocking: θ

Figure 2. Inputs and outputs for evaluating SSI effects in system identification of buildings (Stewart and Fenves 1998).

Butt and Omenzetter

2

First mode
shape

Second
mode shape

Third mode
shape

Y

X

Neutral position .... Base level — — — — — — — · Roof level ————————
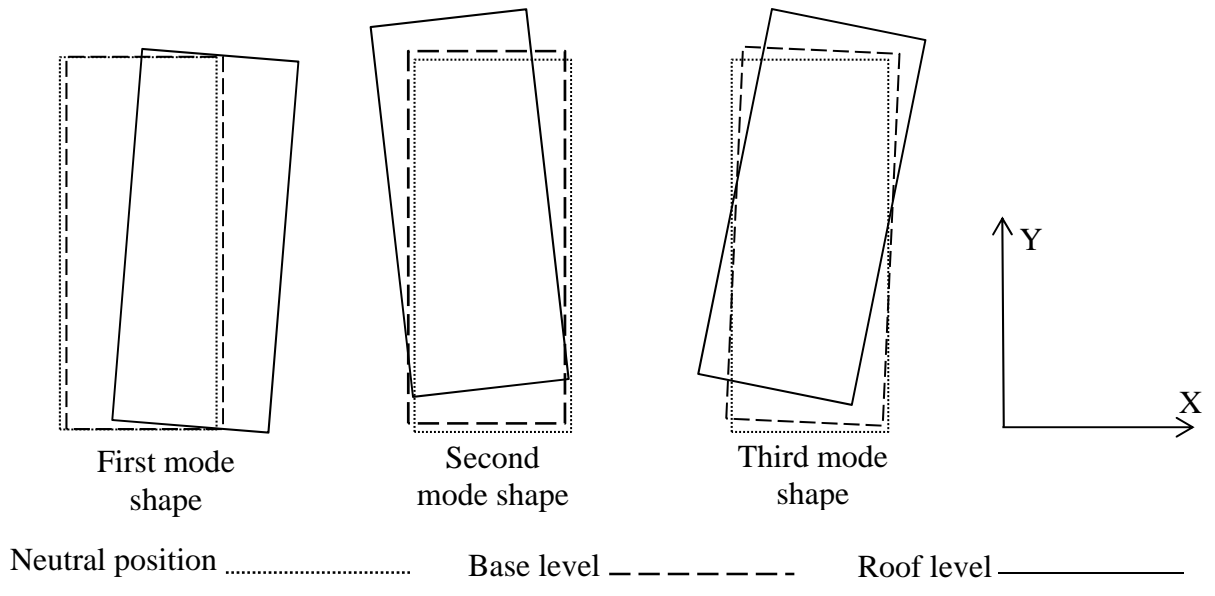
Figure 3. Planar views of the first three mode shapes of the building for flexible base model.

Butt and Omenzetter
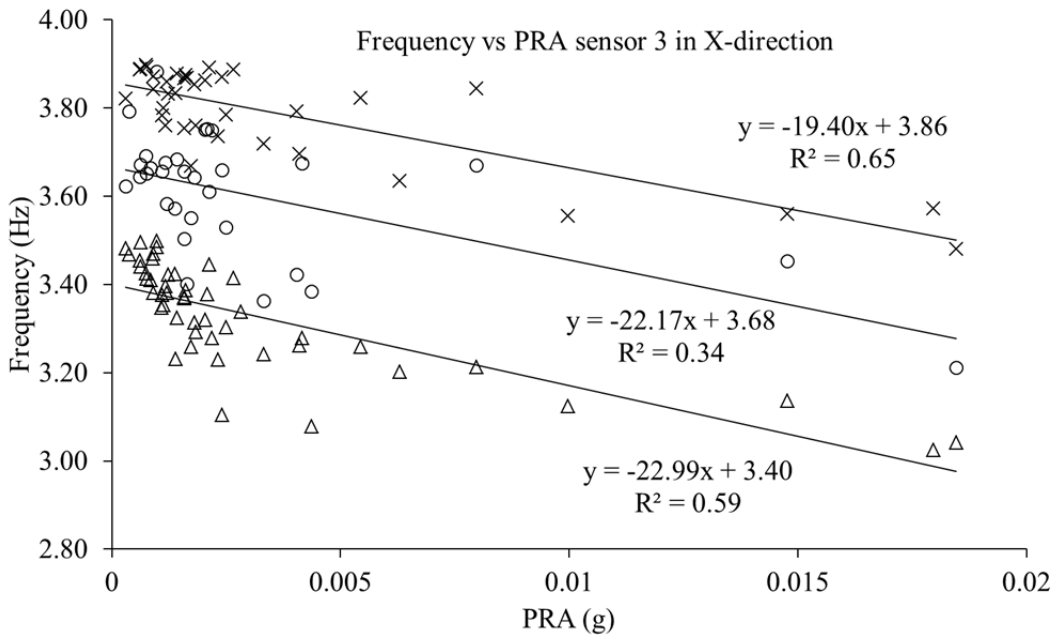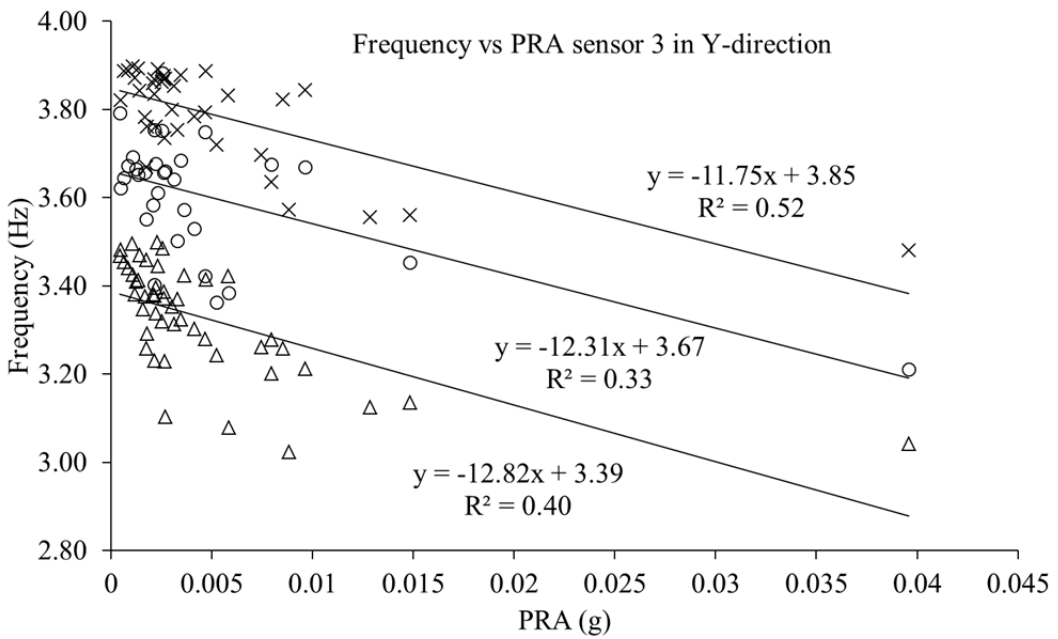
Figure 4. First three modal frequencies of the building for flexible base case vs. PRA of sensor 3: a) X-direction, and b) Y-direction.
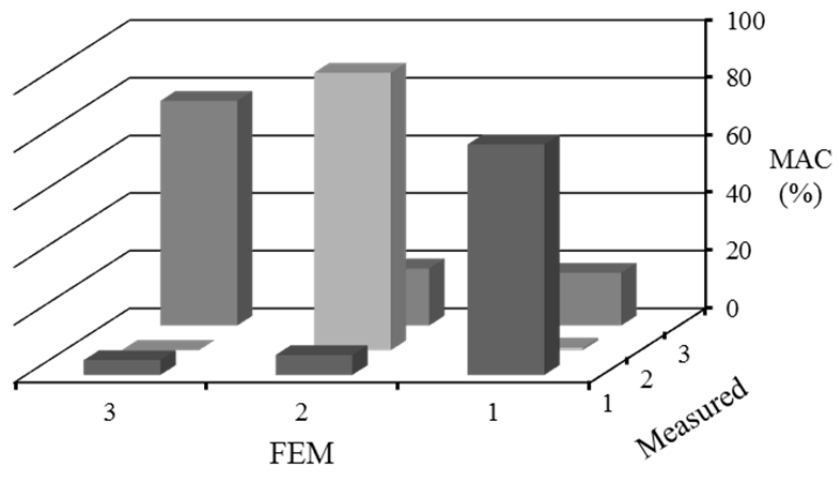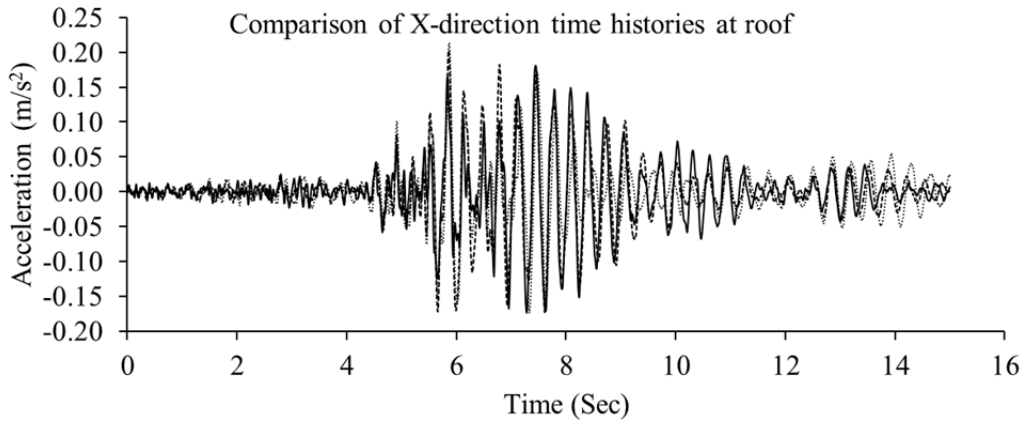
Butt and Omenzetter

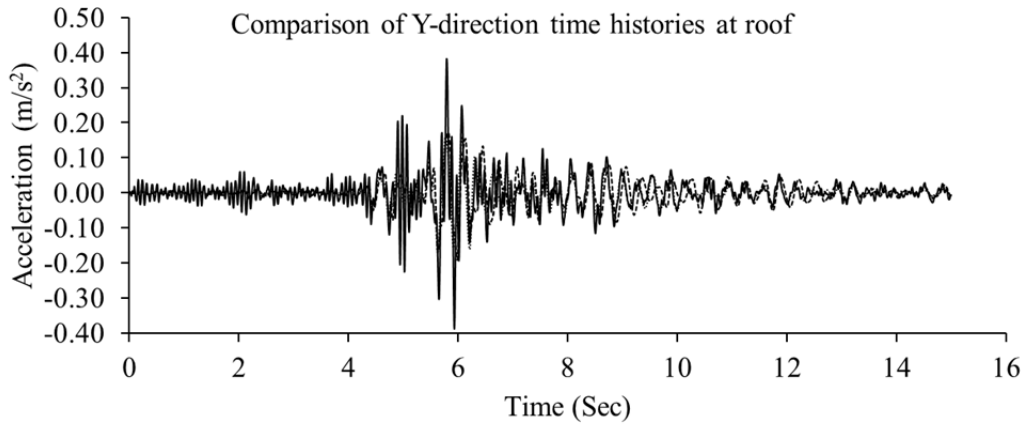Figure 5. MAC matrix between FEM and measured mode shapes: a) initial FEM, and
b) updated FEM.

Butt and Omenzetter

5

First mode
shape

Second mode
shape

Third mode
shape
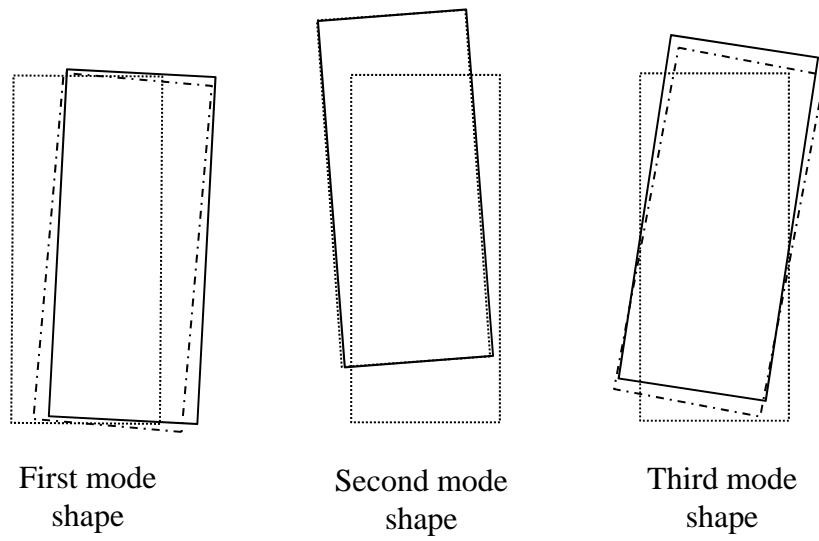
Neutral position ·················· Updated FEM ·-·-·-·-·-·-·- Measured —————

Figure 6. Comparison between mode shapes of the updated FEM and measured
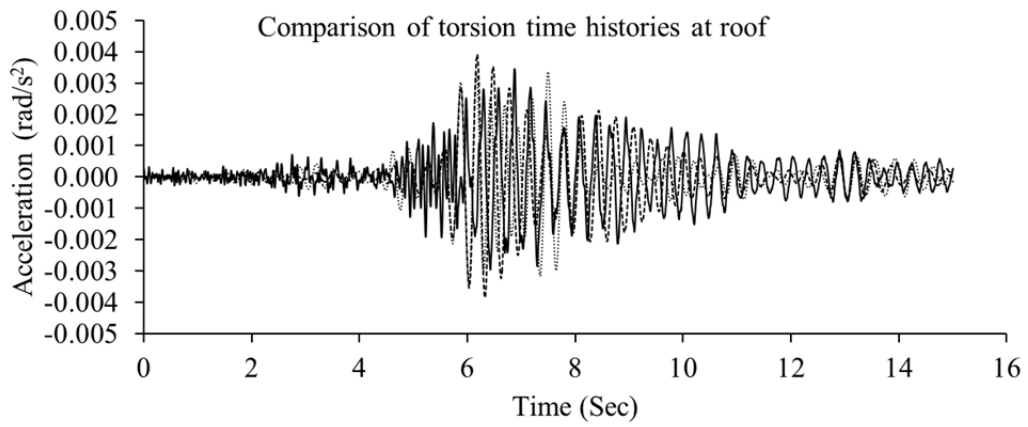
response at the roof level.

Butt and Omenzetter

Figure 7. Recorded and simulated acceleration time histories using initial and updated

FEMs at the roof for the October 10th, 2009 earthquake: a) X-direction, b) Y-

direction, and c) torsion.

Butt and Omenzetter

Comparison of torsion time histories at roof

Actual time history .... Initial time history ------ Updated time history

c)

Figure 7. Recorded and simulated acceleration time histories using initial and updated FEMs at the roof for the October 10th, 2009 earthquake: a) X-direction, b) Y-direction, and c) torsion.
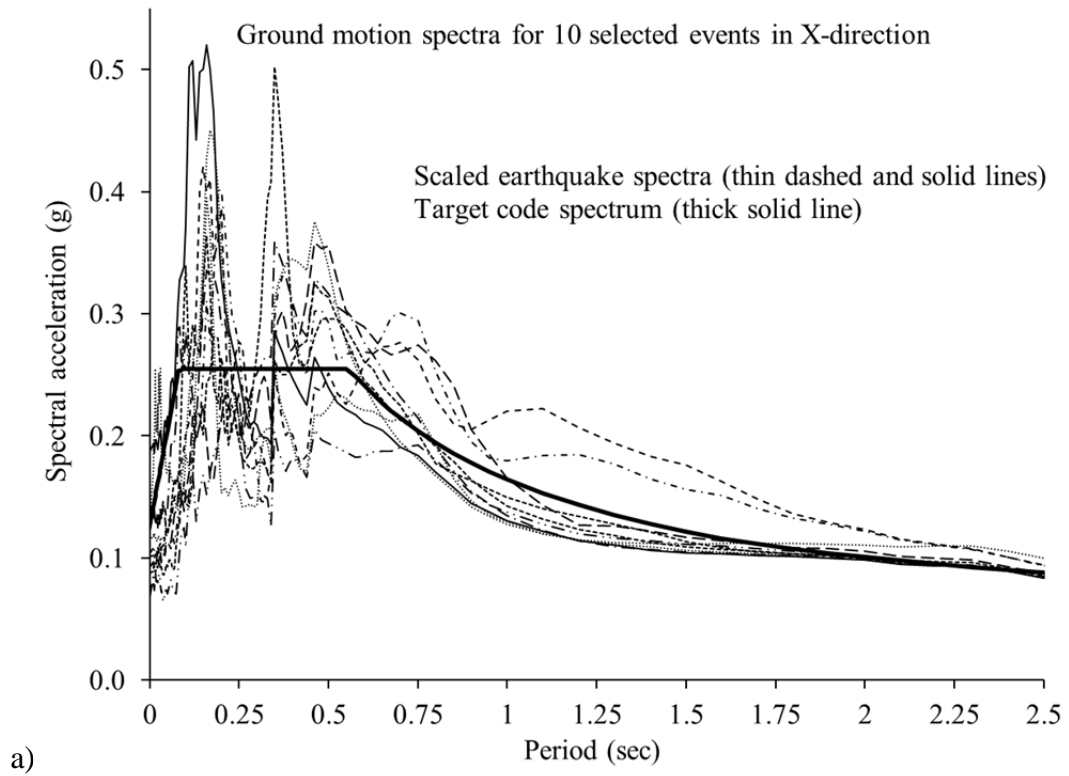
Butt and Omenzetter

8

Figure 8. Target ground motion spectrum from NZS 1170.5:2004 and scaled spectra for 10 seismic events used in serviceability study: a) X-direction, and b) Y-direction.

Butt and Omenzetter

9

Ground motion spectra for 10 selected events in Y-direction

Scaled earthquake spectra (thin dashed and solid lines)
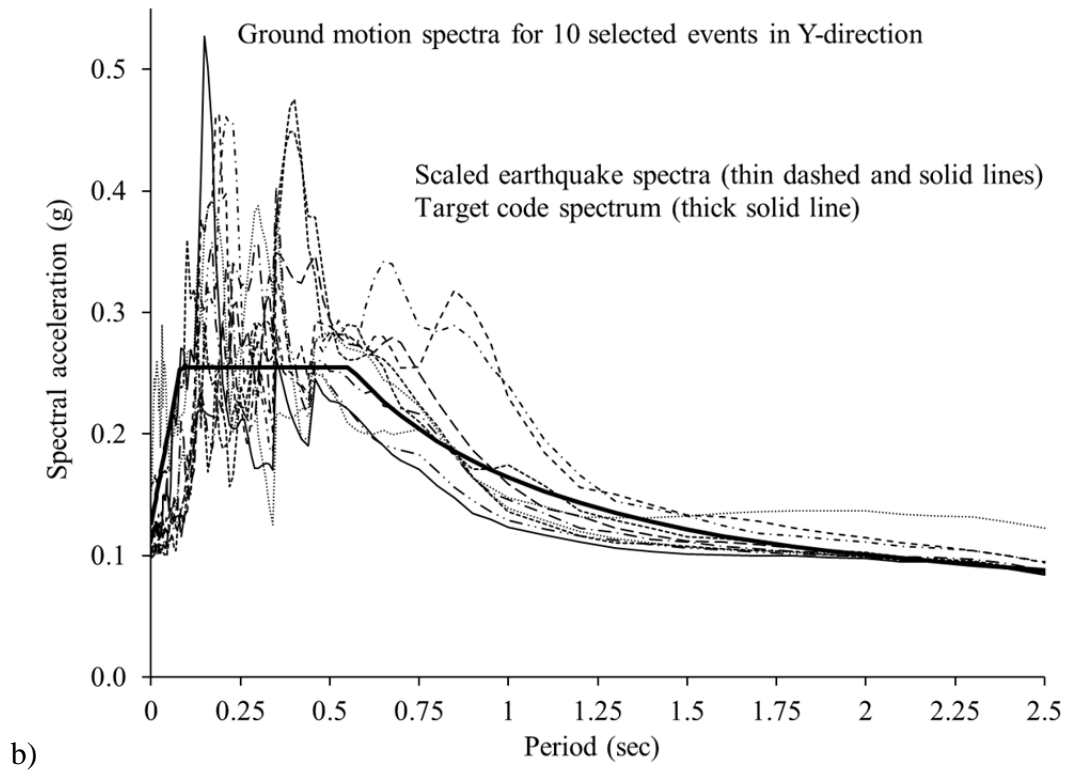Target code spectrum (thick solid line)

b)

Figure 8. Target ground motion spectrum from NZS 1170.5:2004 and scaled spectra

for 10 seismic events used in serviceability study: a) X-direction, and b) Y-direction.

Butt and Omenzetter